

Synthesis, Pharmacokinetics, Efficacy, and Rat Retinal Toxicity of a Novel Mitomycin C-Triamcinolone Acetonide Conjugate

Tamer A. Macky,^{†,‡,||} Carsten Oelkers,^{§,‡} Uwe Rix,[§] Martin L. Heredia,[†] Eva Künzel,[§] Mark Wimberly,[†] Baerbel Rohrer,[†] Craig E. Crosson,[†] and Jürgen Rohr^{*,§}

Department of Ophthalmology and Department of Pharmaceutical Sciences, Medical University of South Carolina, 280 Calhoun Street, Charleston, South Carolina 29425-2301

Received November 5, 2001

A novel conjugate of mitomycin C (MMC) and triamcinolone acetonide (TA) was synthesized using glutaric acid as a linker molecule. To determine the rate of hydrolysis, the conjugate was dissolved in aqueous solution and the rate of appearance of free MMC and TA was determined by high-performance liquid chromatography analysis. Antiproliferative activity of the MMC–TA conjugate and parent compounds was assessed using an NIH 3T3 fibroblast cell line. Cell growth was quantified using the MTT assay. Kinetic analysis of the hydrolysis rate demonstrated that the conjugate had a half-life of 23.6 h in aqueous solutions. The antiproliferative activities of the MMC–TA conjugate and MMC were both concentration dependent, with similar IC_{50} values of 2.4 and 1.7 μ M, respectively. However, individual responses at concentrations above 3 μ M showed that the conjugate was less active than MMC alone. TA alone showed only limited inhibition of cell growth. Studies evaluating intravitreal injection of the conjugate demonstrate that this agent produced no measurable toxicity. Our data provide evidence that the MMC–TA conjugate could be used as a slow-release drug delivery system. This could in turn be used to modulate a posttreatment wound healing process or to treat various proliferative diseases.

Introduction

Mitomycin C (**1**; MMC) is an antitumor antibiotic with an unusual tetracyclic mitosan ring system, including an aziridine ring, a pyrrolizidine ring, a pyrrolo-(1,2a)-indole, and a substituted benzoquinone moiety.^{1–3} Each of these structural elements participates in the unique mechanism-of-action of mitomycin, which is initiated by a reduction of the benzoquinone system leading to a quinone methide covalently binding to DNA and ultimately causing DNA cross-linking and cell death. An initial reduction reaction occurs preferentially in hypoxic cells, which is important for selective antitumor toxicity since many tumors and proliferative disorders are associated with hypoxia.^{3b} In addition, mitomycin can alkylate the DNA at the 2-amino group of guanine nucleosides and cause single-strand breakage of DNA as well as chromosomal breaks. MMC (**1**) is used in combination with other antitumor drugs to treat pancreatic carcinoma as well as lymphatic leukemia.^{4–7} In addition, MMC has applications in ophthalmology, such as postoperative treatment of the pterygium and adjunctive treatment in glaucoma surgery.⁸

Corticosteroids, such as triamcinolone acetonide (**2**; TA), have only limited antiproliferative properties;⁹ however, they may play an important role by preventing the access of inflammatory mediators to a disease site. T-lymphocytes have been, for example, identified in excised membranes from cases of proliferative vitreo-

retinopathy (PVR), which is scar tissue formation in eyes with rheumatogenous retinal detachment.^{10,11} Also, elevated levels of certain cytokines, such as tumor necrosis factor- α (TNF- α)¹² and interleukin-1 (IL-1),¹³ have been found in the vitreous of patients with proliferative disorders. Glucocorticoids inhibit TNF- α and IL-1 expression^{14,15} and can inhibit T-lymphocyte proliferation.¹⁶ Despite the advantages of corticosteroids in the suppression of the inflammatory arm of the wound-healing response, they are limited in their clinical effectiveness because of their weak antiproliferative properties.

The efficacy of antimetabolites and corticosteroids is limited by their short half-life in cavitary organs (e.g., vitreous cavity of the eye). A new slow-delivery system is discussed by Berger and colleagues,¹⁷ utilizing codrug technology. They investigated the use of a 5-fluorouracil and TA conjugate to inhibit experimental PVR in an animal model. In our study, we have investigated a conjugate consisting of MMC and TA. The MMC–TA conjugate (**5**) was synthesized by linking TA and MMC via a glutaric acid unit (Figure 1). In vivo, dissolution of the conjugate followed by hydrolysis allows both active components to be released in an equimolar ratio. We describe the synthesis of the MMC–TA conjugate (**5**), its kinetics, in vitro efficacy, and toxicity to rat retina.

Results

Chemistry. The conjugate of MMC and TA was synthesized in reasonable yields via the route shown in Figure 1. This involved three steps: (i) the catalyzed ketal formation of the secondary (16-OH) and tertiary alcohol (17-OH) groups of triamcinolone with acetone; (ii) the esterification of the primary alcohol (21-OH) of

* To whom correspondence should be addressed. Tel.: (843)876-5091. Fax: (843)792-0759. E-mail: rohrj@musc.edu.

[†] Department of Ophthalmology.

[‡] These authors contributed equally to this work.

[§] Department of Pharmaceutical Sciences.

^{||} New address: Department of Ophthalmology, Cairo University, Cairo, Egypt.

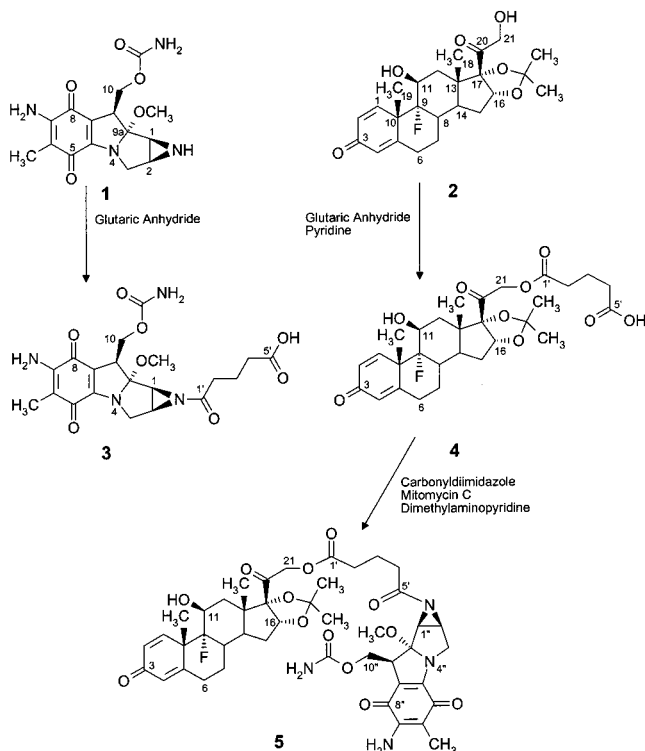


Figure 1. MMC-TA (5) was synthesized from the reaction of TA (2), the TA glutaric acid-linker molecule (4), and MMC (1). For the hydrolysis studies, the MMC glutaric acid-linker molecule (3) was synthesized from the reaction of MMC (1) with glutaric acid.

the resulting TA with the glutaric acid linker using glutaric anhydride and pyridine; and (iii) the amide bond formation between the remaining free, activated (with carbonyl diimidazole) carboxyl group of the glutaric acid linker and the secondary amine group of the aziridine ring of MMC. The resulting MMC-TA conjugate (5) was characterized by mass spectrometry and by 1D and 2D nuclear magnetic resonance (NMR) spectroscopy. All obtained data, in particular NMR long-range couplings (see Discussion), verified the conjugate's structure (5). For comparative reasons, in context with the hydrolysis studies (see later), MMC-glutaric acid amide (3), subsequently called MMC-linker complex, was synthesized from MMC and glutaric anhydride. Structure 3 was verified by its NMR data.

Kinetics and Hydrolysis Studies. In aqueous solutions at pH 7.4, the MMC-TA conjugate was hydrolyzed by cleavage of either the amide bond linking mitomycin and position 5' of the glutaric acid linker or the ester bond linking TA to the 1' position of the linker. Therefore, four different compounds were released, (i) MMC (1), (ii) TA (2), (iii) TA-linker complex (4), and (iv) MMC-linker complex (3). Peaks for MMC, TA, MMC-linker complex, TA-linker complex, and the MMC-TA conjugate were identified by high-performance liquid chromatography (HPLC) through direct comparison with these molecules, which were available from the synthesis outlined above (Figure 1).

Regression analysis of the disappearance of MMC-TA conjugate in aqueous solution demonstrated that the conjugate has a half-life of approximately 23.6 h (Figure 2). Evolution of MMC and the MMC-linker complex (retention times of 3.07 and 3.26 min, respectively) and

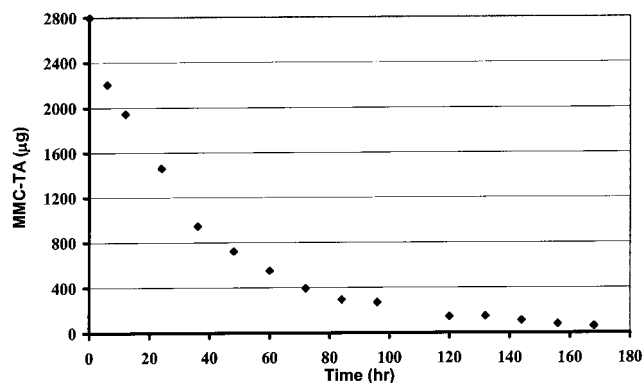


Figure 2. Hydrolysis of the MMC-TA conjugate in 0.1 mol/L phosphate buffer (pH 7.4) and propylene glycol (1:1) is graphically presented.

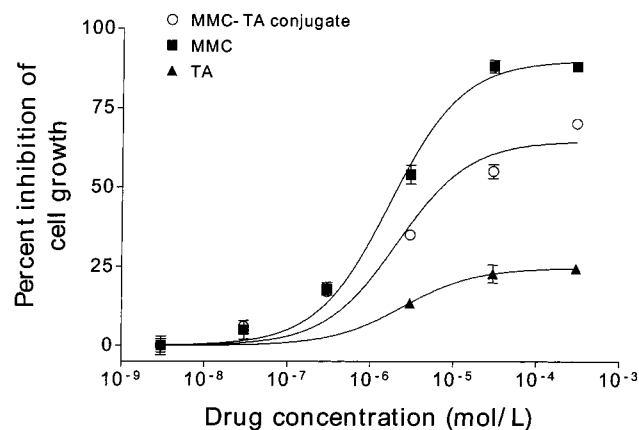


Figure 3. Dose response curve for MMC, TA, and the MMC-TA conjugate, showing different percentages of fibroblast cell growth inhibition (88, 25, and 67%, respectively) when compared to the DMSO similarly treated control.

Table 1. Antiproliferative Assay Results Showing the Maximal Percentage of Fibroblast Cell Growth Inhibition (Response Maximum) and the 50% Inhibitory Concentration (IC_{50}) of MMC, TA, MMC plus TA (1:1, Mixture), and the Conjugate MMC-TA

	IC_{50}^a (μ M)	response maximum (% inhibition)
MMC	1.7	88
MMC-TA conjugate	2.4	67
TA	2.5	25
MMC+TA mixture	1.6	83

^a Concentration required to induce 50% of response maximum.

the evolution of TA and the TA-linker complex (9.73 and 5.71 min, respectively) confirmed the half-life of the conjugate (data not shown).

Antiproliferative Assays. Concentration-response curves for MMC, TA, and the conjugate-induced inhibition of NIH 3T3 cell growth are shown in Figure 3. The calculated response maximums for MMC and the conjugate were 88 and 67%, respectively. The IC_{50} (the concentration required to induce 50% of the response maximum) was calculated to be 1.7 and 2.4 μ M for MMC and the conjugate, respectively (Table 1). The addition of unconjugated MMC and TA together resulted in an inhibitory response similar to that observed with MMC alone (Table 1). The addition of TA alone to the cells produced only limited inhibition of cell growth (25%) at the highest concentration tested.

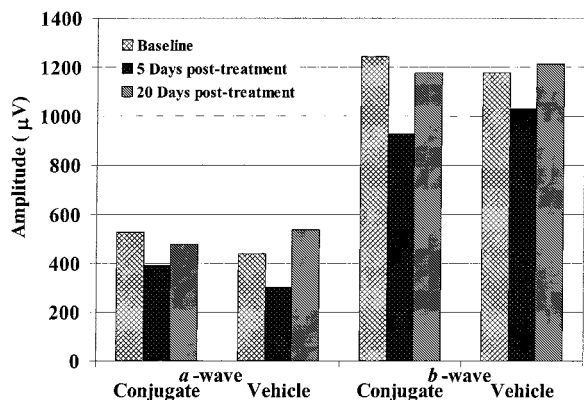


Figure 4. Average amplitudes of the electroretinogram *a*- and *b*-waves before (baseline) and 5 (3 rats) and 20 days (5 rats) postintravitreal injection of the MMC–TA conjugate (right eye) and the DMSO control (left eye).

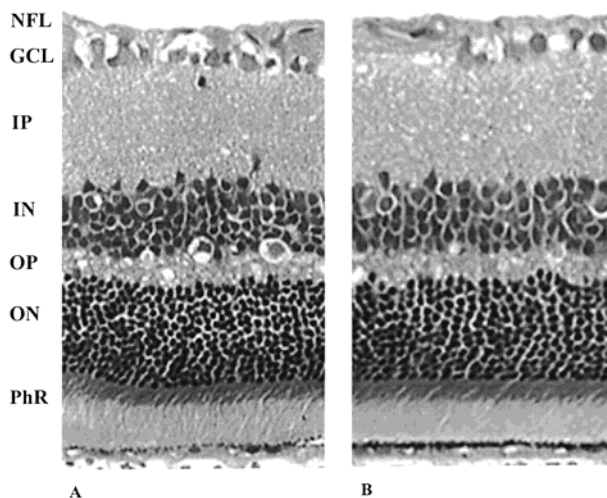


Figure 5. Histopathological sections of the neurosensory retina stained with hematoxylin and eosin ($\times 40$ magnification). (A) Left eye of control (R06) at day 5 postintravitreal injection of 2 μ L, 99.9% DMSO; and (B) right eye of same rat at day 5 postintravitreal injection of 2 μ L 0.39 mg/mL of MMC–TA conjugate. Legend: NFL, nerve fiber layer; GCL, ganglion cell layer; IP, inner plexiform layer; IN, inner nuclear cell layer; OP, outer plexiform layer; ON, outer nuclear cell layer; PhR, photoreceptor cell layer.

In Vivo Toxicity. Electroretinogram. Rats were injected intravitreally (2 μ L) with 0.784 μ g of conjugate or vehicle, and ERG *a*- and *b*-wave amplitudes were analyzed (Figure 4). Eyes that received intravitreal injections of the MMC–TA conjugate (right eyes) were compared to those that received dimethyl sulfoxide (DMSO) only (control, left eyes). There were no statistically significant differences between the amplitudes of the *a*- and *b*-waves at 5 or 20 days posttreatment. The slight reduction in ERG amplitudes observed at 5 days after treatment was attributed to the injection itself, as it affected both eyes equally.

Histopathology. The retina, by light microscopic examination, was normal in appearance at 5 and 20 days following the intravitreal injection of the MMC–TA conjugate, when compared to the DMSO control (Figure 5). No signs of retinal necrosis, photoreceptor cell loss, cystic degeneration, inflammatory cell infiltration, or hypocellularity of nuclear layers were observed microscopically in any rats.

Discussion

Our goal in this study was to link MMC (1) and TA (2) through a C₅ dicarboxylic acid moiety, in which the linker is connected by an ester bond with the primary alcohol function of TA and by an amide bond with the aziridine nitrogen of MMC. Both bonds were anticipated to hydrolyze in aqueous solution at physiological pH. Because the MMC–TA conjugate is a lipophilic molecule, it was expected to dissolve slowly, releasing both active ingredients of this codrug (MMC (1) and TA (2)) over a period of time. The C₅ linker was chosen because it is long enough to avoid sterical hindrance between the two principal building blocks. The glutaric acid linker was first connected to TA. To avoid a reaction of the secondary alcohol group in the 11-position with an excess of glutaric anhydride, only 1.1 equiv of it (relative to TA) was used. The final conversion of the TA linker to the MMC–TA conjugate (5) was easily accomplished by the addition of 3-fold excess of TA linker to MMC. The overall yield (51%) of MMC–TA (relative to MMC) was acceptable, and the procedure was not further optimized. The alternative strategy of attaching the glutaric linker first to MMC was less effective, producing low yields of the MMC–linker molecule (3) needed for the hydrolysis studies.

The conjugation of MMC and TA was confirmed by mass spectrometry and by 1D and 2D NMR spectroscopy. The positive electrospray ionization (ESI) mass spectrum revealed the molecular ion at m/z 887 [MH + Na]⁺, which confirmed the molecular formula of C₄₄H₅₃N₄O₁₃F. The proton NMR spectrum showed all necessary signals, most of which were assigned with the help of the HSQC, HMBC, and H,H-correlation spectroscopy spectra. Also, the ¹³C NMR spectrum showed all expected signals, which were assigned through the ¹J_{C–H} and ⁿJ_{C–H} couplings observed in the HSQC and HMBC spectra. In the HMBC spectrum couplings between C-5' of the linker and the protons attached to C-1' and C-2'' of the mitomycin moiety on one hand and between 21-H₂ and C-1' on the other hand clearly indicated that the linkage of the two compounds occurred in the desired fashion.

The conjugate of MMC and TA was hydrolyzed by cleavage of either the amide bond linking mitomycin and position 1' of the glutaric moiety of the conjugate or the ester bond linking TA and position 1' of the glutaric moiety of the MMC–TA conjugate (Figure 1). As a result, five compounds were identified in these studies: conjugate, TA linker, MMC linker, TA, and MMC. Analysis of the area under the curve (AUC)–time plots demonstrated that the evolution of TA–linker complex occurred faster than the evolution of TA indicating that the amide bond between mitomycin and position 5' of the linker was more easily cleaved than the ester bond between TA and position 1' of the linker. Normally, amide bonds are more stable than ester bonds; however, this is not true for amide bonds whose nitrogen is part of an aziridine ring. Because of the strain on the aziridine ring, the free electron pair of the aziridine nitrogen cannot delocalize freely with the 5'-carbonyl and thus cannot contribute to a +M effect, which would normally decrease the reactivity of the amide C-5' carbonyl.¹⁸

Once most of the conjugate had been hydrolyzed, the amount of TA linker decreased slightly due to cleavage of the ester bond between the TA and the linker. This is in agreement with the observed steady increase in the concentration of TA, even after most of the original TA-MMC conjugate had been hydrolyzed. The cleavage of this ester bond, however, appeared to be slower once the amide bond had been broken, since changes in the amounts of the compounds were only slight.

Similar quantitative observations could not be made for MMC and the mitomycin linker, since we were unable to completely separate their peaks by HPLC. The AUC of the combined peaks was fairly constant, once most of the conjugate had been hydrolyzed; thus, one can assume that mitomycin was reasonably stable under these conditions (aside from the conversion of mitomycin-linker complex to mitomycin). A control study supported this view, in which pure mitomycin was dissolved in phosphate buffer and propylene glycol to analyze the behavior of the compound under the same conditions as those used in the kinetic assay. Samples were taken every 24 h and analyzed by HPLC showing that no additional peaks (in addition to the mitomycin peak) appeared and the AUC of the single peak was fairly constant.

In the antiproliferative assay study, the MMC-TA conjugate and MMC showed a concentration-dependent antiproliferative activity at concentrations from 0.03 to 30 μM . The IC_{50} values for MMC and the MMC-TA conjugate were 1.7 and 2.4 μM , respectively. Although regression analysis demonstrated that the IC_{50} for MMC and the conjugate was not significantly different, the individual responses at concentrations above 3 μM , as well as the response maximum, were significantly less ($p < 0.05$) for the conjugate when compared to the parent MMC compound at the same concentration. We also compared the parent MMC response curve to the coadministration of equal molar concentrations of MMC and TA to determine if there were any interactions between the two drugs (MMC and TA) that contributed to the decreased efficacy of the conjugate. Although a slight difference between MMC (88%) in comparison to the MMC+TA mixture (83%) was observed, it could not alone explain the decreased efficacy of the conjugate. Hence, this reduction in conjugate activity at high concentrations is likely due to the conjugates limited activity before hydrolyzing and releasing the parent compounds, MMC and TA.

Intravitreal administration of the conjugate revealed no evidence of toxicity by ERG evaluation or histopathologic examination. The total ocular dose administered to these animals was approximately equivalent to the maximum effective concentration identified in the cell proliferation assay. These initial data support the idea that this MMC-TA conjugate will be relatively safe for various proliferative diseases including inflammatory and neoplastic disorders.

In summary, the newly synthesized MMC-TA conjugate (**5**) appeared to have similar hydrolysis kinetics as the previously described 5-FU-TA conjugate.^{10,17} The conjugate also showed sufficient antiproliferative activity of the released compounds (MMC and TA) after its hydrolysis. The idea of using MMC in combination with triamcinolone was suggested after both agents were

found to be effective in treating experimental proliferative ocular diseases,¹⁹⁻²¹ thus taking advantage of the best characteristics of these two agents while minimizing their individual liabilities. The drugs become relatively insoluble when linked together. Hydrolysis of the conjugate allows the MMC and TA to be released slowly in equimolar concentrations. Ideally, a sustained drug delivery system should release the drug over a prolonged period of time, corresponding to the duration of disease activity. Our data suggest that the MMC-TA conjugate pharmacokinetics profile would be advantageous in the treatment of proliferative diseases affecting cavitary organs, where the short half-life of these agents has limited their clinical use.

Experimental Section

TA (2).²² Triamcinolone, 800 mg (2.03 mmol), was suspended in 200 mL of acetone, and 20 drops of concentrated hydrochloric acid were added. The mixture was stirred under reflux for 1 h, during which triamcinolone was completely dissolved. The solution was stirred at room temperature for another 17 h. Thereafter, the mixture was poured into a solution of sodium bicarbonate (1 g/100 mL) and extracted with ethyl acetate. The combined organic layers were washed with a saturated sodium chloride solution, dried over potassium carbonate, and evaporated to dryness. Purification of the crude product was accomplished by column chromatography (silica, methylene chloride/methanol: 15/1) yielding TA (**2**), 458 mg (1.05 mmol; 52%), as a white solid; mp 275 °C (dec); R_f 0.42 ($\text{CH}_2\text{Cl}_2/\text{CH}_3\text{OH}$ 15:1). ^1H NMR (400 MHz, acetone- d_6): δ 7.30 (d, $J = 10$, 1H, 1-H), 6.21 (dd, $J = 10$, $J = 2$, 1H, 2-H), 6.02 (dd, $J = 2$, $J = 2$, 1H, 4-H), 5.00 (dd, $J = 3$, $J = 2$, 1H, 16-H), 4.65 (dd, $J = 9$, $J = 4$, 1H, 21-H), 4.51 (s, 1H, exchangeable by D_2O , 11-OH), 4.40 (dddd, $J = 11$, $J = 4$, $J = 3$, $J = 2$, 1H, 11-H), 4.16 (dd, $J = 9$, $J = 3$, 1H, 21-H), 3.89 (br s, 1H, exchangeable by D_2O , 21-OH), 2.74 (dddd, $J = 14$, $J = 14$, $J = 6$, $J = 2$, 1H, 6-H), 2.60 (dddd, $J = 29$, $J = 12$, $J = 12$, $J = 5$, 1H, 8-H), 2.39 (ddd, $J = 14$, $J = 5$, $J = 2$, 1H, 6-H), 2.21 (ddd, $J = 14$, $J = 4$, $J = 4$, 1H, 12-H_a), 2.08 (m, 1H, 14-H), 1.93 (ddd, $J = 14$, $J = 6$, $J = 6$, 1H, 7-H_a), 1.73 (dd, $J = 14$, $J = 2$, 1H, 12-H_a), 1.63 (m, 1H, 15-H), 1.62 (s, 1H, 19-H), 1.50 (dddd, $J = 14$, $J = 14$, $J = 14$, $J = 5$, 1H, 7-H_b), 1.39 (s, 3H, acetonide- CH_3), 1.13 (s, 3H, acetonide- CH_3), 0.90 (s, 1H, 18-H). ^{13}C NMR (100.6 MHz, acetone- d_6): δ 210.8 (s, 20-H), 185.9 (s, C-3), 166.5 (s, C-5), 152.5 (d, C-1), 130.2 (d, C-2), 125.5 (d, C-4), 111.7 (s, $\text{C}(\text{CH}_3)_2$), 101.3 (d, C-9), 98.2 (d, C-17), 82.3 (d, C-16), 72.2 (dd, C-11), 67.4 (t, C-21), 48.9 (d, C-10), 45.9 (s, C-13), 44.1 (d, C-14), 37.4 (t, C-6), 34.1 (t, C-7), 33.9 (dd, C-8), 31.3 (t, C-12), 28.5 (t, C-15), 26.7 (q, acetonide- CH_3), 25.6 (q, acetonide- CH_3), 23.6 (q, C-19), 17.0 (q, C-18). UV (CH_3OH) λ_{max} (ϵ): 238 (18 400), 201 (10 300), 192 (7400). MS (pos.-APCI) m/z 435 M^+ (100).

TA-Glutaric Acid Linker (4).²² TA, 260 mg (0.60 mmol), and glutaric anhydride, 78.0 mg (0.68 mmol), 1.13 equiv referred to TA, were placed into a 10 mL flask that had been previously flushed with argon. Then, 2.5 mL of dried pyridine was added, after which the mixture was stirred at room temperature for 18 h. The mixture was poured into 50 mL of ice water and acidified with 10% hydrochloric acid. After extraction with methylene chloride, the combined organic layers were evaporated to dryness, using toluene to remove the remaining pyridine. Purification of the crude product was accomplished by column chromatography (silica, methylene chloride/methanol: 15/1) to yield 268 mg (0.49 mmol, 83%) of TA linker (**4**) as a white solid; mp 220 °C (dec); R_f 0.23 ($\text{CH}_2\text{Cl}_2/\text{CH}_3\text{OH}$ 15:1). ^1H NMR (400 MHz, acetone- d_6): δ 7.31 (d, $J = 10$, 1H, 1-H), 6.22 (dd, $J = 10$, $J = 2$, 1H, 2-H), 6.02 (s, 1H, 4-H), 5.15 (d, $J = 18$, 1H, 21-H), 4.94 (m, 1H, 16-H), 4.81 (d, $J = 18$, 1H, 21-H), 4.66 (br s, 1H, exchangeable by D_2O , 11-OH), 4.44 (m, 1H, 11-H), 2.75 (dddd, $J = 14$, $J = 14$, $J = 8$, $J = 2$, 1H, 6-H), 2.61 (dddd, $J = 29$, $J = 12$, $J = 12$, $J = 5$, 1H, 8-H), 2.42 (t, $J = 7$, 2H, 2'- or 4'-H₂), 2.52 (t, $J = 7$, 2H, 2'- or 4'-H₂), 2.39 (ddd, $J = 14$, $J = 6$, $J = 2$, 1H, 6-H), 2.25 (ddd, J

= 14, $J = 3$, $J = 3$, 1H, 12-H_c), 2.08 (m, 1H, 14-H), 1.93 (m, obscured by 3'-H, 1H, 7-H_a), 1.93 (t, $J = 7$, 2H, 3'-H₂), 1.84 (dd, $J = 14$, $J = 2$, 1H, 12-H_a), 1.68 (m, 1H, 15-H), 1.63 (s, 1H, 19-H), 1.50 (dddd, $J = 13$, $J = 13$, $J = 13$, $J = 5$, 1H, 7-H_b), 1.41 (s, 3H, acetone-CH₃), 1.20 (s, 3H, acetone-CH₃), 0.94 (s, 1H, 18-H). ¹³C NMR (100.6 MHz, acetone-*d*₆): δ 204.3 (s, 20-H), 186.1 (s, C-3), 174.2 (s, C-1'), 173.0 (s, C-5'), 166.7 (s, C-5), 152.6 (d, C-1), 130.3 (d, C-2), 125.6 (d, C-4), 112.2 (s, C(CH₃)₂), 101.5 (d, C-9), 98.5 (d, C-17), 82.6 (d, C-16), 72.3 (dd, C-11), 68.1 (t, C-21), 49.0 (d, C-10), 46.4 (s, C-13), 44.2 (d, C-14), 37.4 (t, C-6), 34.4 (t, C-7), 34.1 (dd, C-8), 33.3 (t, C-2'), 33.1 (t, C-4'), 31.5 (t, C-12), 28.6 (t, C-15), 26.9 (q, acetone-CH₃), 26.0 (q, acetone-CH₃), 23.8 (q, C-19), 21.1 (t, C-3'), 16.9 (q, C-18). UV (CH₃OH) λ_{\max} (ϵ): 238 (14 200), 200 (6800), 195 (6300), 191 (6000). MS (pos.-APCI) m/z 549 M⁺ (100).

MMC-TA Conjugate (5).^{17,22,23} A total of 216 mg (0.39 mmol) of TA linker and 65.0 mg (0.40 mmol, 1.02 equiv referred to TA linker) of carbonyldiimidazole (CDI) were dissolved in 3 mL of dried tetrahydrofuran (THF) (under argon), and the solution was stirred at room temperature for 4 h. Then, 37.0 mg (0.11 mmol, 0.29 equiv referred to TA linker) of MMC (Bristol Myers Squibb Oncology, Princeton, New Jersey) and 3 mg of (dimethylamino)pyridine (DMAP) were added, and the mixture was stirred at room temperature for 4 days. The reaction mixture was poured into 50 mL of water and extracted 3 times with chloroform. The combined organic layers were washed with water, dried over sodium sulfate, and evaporated to dryness. Purification of the crude product was accomplished by column chromatography (silica, chloroform/methanol: 10/1) to yield 59 mg (0.07 mmol, 43%) of the MMC-TA conjugate (5) as a purple solid. The purity of the compound was verified by two different HPLC gradient systems (system 1: R_{rel} 12.8 min, H₂O/CH₃CN/CH₃OH = 70%:24%:6% to H₂O/CH₃CN/CH₃OH = 50%:40%:10% within 5 min; system 2: R_{rel} 3.4 min, H₂O/CH₃CN/CH₃OH = 45%:45%:10% to H₂O/CH₃CN/CH₃OH = 0%:83%:17% within 10 min; Waters Nova-Pak C₁₈ 3.9 mm \times 150 mm, flow rate for both systems: 1.5 mL/min). R_f 0.31 (CHCl₃/CH₃OH 15:1). ¹H NMR (400 MHz, CDCl₃): δ 7.26 (d, $J = 10$, 1H, 1-H), 6.35 (dd, $J = 10$, $J = 2$, 1H, 2-H), 6.12 (br s, 1H, 4-H), 5.38 (br s, 2H, 7''-NH₂ or CONH₂), 5.09 (br s, 2H, 7''-NH₂ or CONH₂), 4.96 (d, $J = 5$, 1H, 16-H), 4.80–4.94 (m, complex, 3H, 10''-H and 21-H₂), 4.44 (m, obscured by 3'-H, 1H, 11-H), 4.44 (d, $J = 13$, 1H, 3''-H), 4.04 (dd, $J = 11$, $J = 11$, 1H, 10''-H), 3.67 (dd, $J = 11$, $J = 5$, 1H, 9''-H), 3.56 (dd, $J = 13$, $J = 2$, 1H, 3''-H), 3.51 (d, $J = 5$, 1H, 1''-H), 3.37 (dd, $J = 5$, $J = 2$, 1H, 2''-H), 3.20 (s, 3H, 9a''-OCH₃), 2.65 (m, 6-H), 2.48 (m, 2H, 2''-H₂), 2.46 (m, 2H, 4''-H₂), 2.40 (m, 1H, 6-H), 2.35 (m, 1H, 12-H), 2.10 (m, 1H, 14-H), 1.95 (ddd, $J = 7$, $J = 7$, $J = 7$, 2H, 3''-H₂), 1.85 (m, obscured, 1H, 7-H), 1.78 (s, 3H, 6''-CH₃), 1.75 (m, 1H, 12-H), 1.65 (m, 1H, 8-H), 1.60 (m, 1H, 15-H), 1.60 (m, 1H, 7-H), 1.55 (s, 1H, 19-H), 1.42 (s, 3H, acetone-CH₃), 1.19 (s, 3H, acetone-CH₃), 0.94 (s, 1H, 18-H). ¹³C NMR (100.6 MHz, CDCl₃): δ 204.0 (20-H), 186.2 (C-3), 183.0 (C-5'), 178.2 (C-5''), 175.2 (C-8''), 172.4 (C-1'), 166.0 (C-5), 156.6 (CONH₂), 154.0 (C-4a''), 152.0 (C-1), 147.2 (C-7''), 130.0 (C-2), 125.0 (C-4), 111.6 (C(CH₃)₂), 110.0 (C-8a''), 105.7 (C-9a''), 105.6 (C-6''), 100.1 (d, C-9), 97.8 (C-17), 82.0 (C-16), 72.1 (d, C-11), 68.0 (C-21), 62.0 (C-10''), 52.0 (C-9''), 50.0 (9a''-OCH₃), 49.0 (d, C-10), 49.0 (C-3'), 45.8 (C-13), 43.4 (C-14), 42.8 (C-1'), 39.8 (C-2''), 37.6 (C-12), 35.4 (C-4'), 34.1 (C-15), 33.8 (C-8), 33.5 (C-2'), 31.5 (C-6), 27.8 (C-7), 26.2 (acetone-CH₃), 26.0 (acetone-CH₃), 23.0 (C-19), 19.8 (C-3'), 16.3 (C-18), 8.0 (6''-CH₃). UV (CH₃OH) λ_{\max} (ϵ): 356 (16 600), 234 (19 700), 212 (22 400). MS (pos.-ESI) m/z 887 (40) [M - H + Na]⁺, H_R calcd for C₄₄H₅₃N₄O₁₃FN_a, 887.3491; found, 887.3489, 833 (100) [M - H - OCH₃]⁺.

Mitomycin-Glutaric Acid Linker (3). A 37.1 mg (0.11 mmol) amount of MMC was dissolved in 4 mL of dry THF under an argon atmosphere and treated with 14 mg (0.12 mmol, 1.1 equiv relative to MMC) of glutaric anhydride. After the solution was stirred for 72 h at room temperature, the solution was poured on ice, acidified with diluted hydrochloric acid, and extracted with chloroform. Purification was achieved by chromatography ((1) silica, CH₃OH. (2) Sephadex LH 20,

CH₃OH) to yield 4 mg (8%) of MMC linker (3) as a purple solid. ¹H NMR (400 MHz, acetone-*d*₆): 6.39 (br s, exchangeable with CD₃OD, 2H, 7-NH₂ or CONH₂), 5.99 (br s, exchangeable with CD₃OD, 2H, 7-NH₂ or CONH₂), 4.95 (dd, $J = 11$, $J = 4$, 1H, 10-H), 4.43 (d, $J = 14$, 1H, 3-H), 3.98 (dd, $J = 11$, $J = 11$, 1H, 10-H), 3.65 (dd, $J = 11$, $J = 4$, 1H, 9-H), 3.59 (d, $J = 5$, 1H, 1-H), 3.48–3.53 (m, complex, 2H, 2-H and 3-H), 3.20 (s, 3H, 9a-OCH₃), 2.42–2.62 (m, 2H, 2''-H₂), 2.30 (t, $J = 7$, 2H, 4''-H₂), 1.82 (m, 2H, 3''-H₂), 1.80 (s, 3H, 6-CH₃).

Kinetics and Hydrolysis Studies. To determine its hydrolysis rate, 2.8 mg (3.3×10^{-6} mol) of the MMC-TA conjugate was dissolved in 2 mL of 0.1 M phosphate buffer (pH 7.4) and 2 mL of propylene glycol (PG).^{24–26} The addition of PG was necessary to increase the solubility of the MMC-TA conjugate. The resulting solution was incubated at 37 °C. Samples of 25 μ L each were taken after 6 and 12 h and each 12 h thereafter. The samples were immediately injected into the HPLC to study the hydrolysis of the conjugate. To determine absolute quantities of the hydrolysis fragments, four calibration curves were made available using pure MMC, MMC-TA conjugate, TA, TA linker, and MMC linker.

HPLC System. Column: M & W Chromatographietechnik Kromasil 100 C18, 250 mm \times 4.6 mm, 5 μ m; flow: 1 mL/min; mobile phase: methanol/water: 60/40 \rightarrow methanol/water: 100/0 within 16 min, then methanol/water: 60/40 for 4 min; detection of the compounds at wavelengths of $\lambda = 234$ nm for MMC, TA, and TA linker; and $\lambda = 356$ nm for the MMC-TA conjugate.

The areas for the observed peaks were determined and plotted in an AUC-time plot. Because the two peaks for mitomycin and mitomycin linker could not be separated by HPLC, their AUCs were added and plotted in one plot. AUCs for the evolution of MMC were therefore not converted to absolute amounts (mg). Because of injection of the samples in a different solvent than was used for the calibration curves, the retention times changed somewhat but were verified by injecting pure samples of the compound in the same solvent. To study the behavior of pure mitomycin under the same conditions, mitomycin was dissolved in phosphate buffer and PG and also incubated at 37 °C. Samples were taken every 24 h and analyzed by HPLC.

Antiproliferative Assay. The fibroblast cell line (NIH 3T3) was cultured in Dulbecco's modified Eagles' medium containing 10% fetal bovine serum. Cells were plated at a density of 100 000 cells/well and allowed to grow for 24 h at 37 °C in 5% carbon dioxide in air.

The MMC-TA conjugate, MMC, and TA were dissolved in DMSO and diluted with media to achieve a final concentration between 3.0×10^{-4} and 3.0×10^2 μ M. Each experiment was performed in triplicate. Cell proliferation was determined by means of the 3-[4,5-dimethylthiazol-2-yl]-2,5-diphenyl tetrazolium bromide (MTT) assay (Roche Molecular Biochemical; Mannheim, Germany). The assay was conducted according to the manufacturer's recommendations. MTT assay samples were measured using a spectrophotometer at an absorbance wavelength of 560 nm and a reference wavelength of 650 nm.

Toxicity to Rat Retina. Eight Wistar female rats, 4-weeks-old and weighing 70 g each, were used in this part of the study. Toxicity of the MMC-TA conjugate was assessed in response to intravitreal injections, using both functional (scotopic ERG) and anatomical (histopathology) analyses.

Our animal study was approved by the Institutional Animal Care and Use Committee. Research animal care and use at our institution meets all USDA and AAALAC approval requirements. Our study protocol adhered to the Association for Research in Vision & Ophthalmology Statement regarding the Use of Animals in Ophthalmic and Vision Research.

Intavitreal Injections. Two microliters containing 0.784 μ g of MMC-TA conjugate dissolved in absolute DMSO was injected into the vitreous through the pars plana, under visualization with a microscope, following a paracentesis. This exposed the intraocular tissues to a concentration of approximately 30 μ M of the MMC-TA conjugate, assuming a rat vitreous volume of 30 μ L. The right eye of each rat received

the conjugate, while the fellow eye (left eye) received an intravitreal injection of 2 μ L of DMSO and served as the control.

Electroretinogram. Animals were dark-adapted overnight and anesthetized with ketamine (11 mg/kg) and xylazine (14 mg/kg), their pupils were dilated with 1% atropine, and their corneas were anaesthetized with topical eye drops (0.5% proparacaine hydrochloride).

Setup. The optical system was adapted from Lyubarsky and Pugh²⁷ as described in Rohrer et al.²⁸ A clear plastic holder ending in a curved tip the shape of the cornea was used to provide full-field light stimulation to the rat's retina via a fiber optic light guide. The diffuser element, which had a recording electrode (0.2 mm platinum wire) glued to the inside, was gently placed against the cornea and electrical contact was completed through a drop of methylcellulose. Tungsten needle electrodes were placed in the neck and tail, to serve as reference and ground. Responses were amplified 2000-fold, band-pass filtered at 0.1–1000 Hz (2 pole Butterworth filter), and digitized with a 12 bit analogue to digital converter at 2 Hz. Data were stored, displayed, and analyzed with a PC interface and PClamp software. A single-channel optical bench was used for light stimulation.

Light Stimulus. The optical pathway consisted of a 250 Watt halogen lamp, and focusing lenses were used to focus the light beam to the end of the liquid light guide, a 500 nm band-pass filter, and a mechanical shutter. ERGs were recorded in response to 10 ms flashes at 40% maximum light intensities. Two responses were averaged, and the time between flashes was set to allow recovery of the *b*-wave between flashes.

Data Analysis. Flash ERGs were recorded prior to intraocular drug administration, to establish a baseline for *a*- and *b*-wave amplitudes, and 5 and 20 days after treatment. The *a*- and *b*-waves of the DMSO-injected eyes (left eyes) and drug-injected eyes (right eyes) were averaged (\pm standard error of the mean), and for statistical purposes, a standard *T*-test was employed, accepting a significance level of $p < 0.05$.

Histopathology. The eight female rats used for ERG analysis were euthanized (0.3 mL pentobarbital) at 5 days (3 rats) and 20 days (5 rats) for histopathological analyses. The animals were deeply anesthetized, and their eyes were enucleated and immediately immersed in a fixative consisting of 10% buffered formaldehyde solution and later processed in paraffin. Sections were stained with hematoxylin and eosin, and the coverslip was secured with DPX for light microscopy examination.

Acknowledgment. This work was supported by the Medical University of South Carolina, Institutional Research funds, 1999–2000; the South Carolina Commission of Higher Education; the U.S. Department of Defense; Research to Prevent Blindness; and NIH EY09741 (C.E.C.). The clinical expertise of D. Virgil Alfaro II, M.D., Farrow Counts, M.S., Todd Shearer, Ph.D., and Enrique-Roig, M.D., is gratefully acknowledged. The authors have no financial or proprietary interest in the products or equipment herein.

References

- Stevens, C. L.; Taylor, K. G.; Munk, M. E.; Marshall, W. S.; Noll, K.; Shah, G. D.; Shah, L. G.; Uzu, K. Chemistry and Structure of Mitomycin C. *J. Med. Chem.* **1965**, *8*, 1–10.
- Fukuyama, T.; Nakatsubo, F.; Cocuzza, A. J.; Kishi, Y. Synthetic Studies Toward Mitomycins. III. Total Syntheses of Mitomycins A and C. *Tetrahedron Lett.* **1977**, 4295–4298.
- (a) Fukuyama, T.; Yang, L. Practical Total Synthesis of Mitomycin C. *J. Am. Chem. Soc.* **1989**, *111*, 8303–8304. (b) Sartorelli, A. C.; Hodnick, W. F.; Belcourt, M. F.; Tomasz, M.; Haffty, B.; Fischer, J. J.; Rockwell, S. *Oncology Res.* **1994**, *6*, 501–508.
- Goodman & Gilman's The Pharmacological Basis of Therapeutics*, 9th ed.; Hardman, J. G., Limbird, L. E., Molinoff, P. B., Ruddon, R. W., Gilman, A. G., Eds.; McGraw-Hill: New York, 1996; pp 1268–1269.
- Beijnen, J. H.; Bult, A.; Underberg, W. J. M. Mitomycin C. *Anal. Profiles Drug Subst.* **1986**, *16*, 361–401.
- Verweij, J.; Schellens, J. H. M.; Loo, T. L.; Pinedo, H. M. Antitumor Antibiotics. In *Cancer Chemotherapy: Principles and Practice*, 2nd ed., Chabner, B. A., Longo, D. L., Eds.; J. B. Lippincott Co: Philadelphia, 1995; pp 395–407.
- Crooke, S. T. Antitumor Antibiotics II: Actinomycin D, Bleomycin, Mitomycin C and Other Antibiotics. In *The Cancer Pharmacology Annual*; Chabner, B. A., Pinedo, H. M., Eds.; Excerpta Medica: Amsterdam, 1983; pp 69–79.
- Mahar, P. S.; Nwokora, G. E. Role of Mitomycin C in Pterygium Surgery. *Br. J. Ophthalmol.* **1993**, *77*, 433–435.
- Ruhmann, A.; Berliner, D. Effect of Steroids on Growth of Mouse Fibroblasts In Vitro. *Endocrinology* **1965**, *76*, 916–927.
- Charteris, D. G.; Hiscott, P.; Grierson, I.; Lightman, S. L. Proliferative Vitreoretinopathy: Lymphocytes in Epiretinal Membranes. *Ophthalmology* **1992**, *99*, 1364–1367.
- Charteris, D. G.; Hiscott, P.; Robey, H. L.; Gregor, Z. J.; Lightman, S. L.; Grierson, I. Inflammatory Cells in Proliferative Vitreoretinopathy Subretinal Membranes. *Ophthalmology* **1993**, *100*, 43–46.
- Little, B. C.; Limb, G. A.; Meager, A.; Ogilvie, J. A.; Wolstencroft, R. A.; Fraks, W. A.; Chignell, A. H.; Dumonde, D. C. Cytokines in Proliferative Vitreoretinopathy. *Invest. Ophthalmol. Visual Sci.* **1991**, *32*, 768.
- Limb, G. A.; Little, B. C.; Meager, A.; Ogilvie, J. A.; Wolstencroft, R. A.; Fraks, W. A.; Chignell, A. H.; Dumonde, D. C. Cytokines in Proliferative Vitreoretinopathy. *Eye* **1991**, *5*, 686–693.
- Schleimer, R. P. An Overview of Glucocorticoids Antiinflammatory Actions. *Eur. J. Clin. Pharmacol.* **1993**, *45*, S3–S7.
- Lee, S. W.; Tsou, A. P.; Chan, H.; Thomas, J.; Petrie, K.; Eugui, E. M.; Allison, A. C. Glucocorticoids Selectively Inhibit the Transcription of the Interleukins 1B Gene and Decrease the Stability of Interleukins 1B mRNA. *Proc. Natl. Acad. Sci. U.S.A.* **1988**, *85*, 1204–1208.
- Arya, S. K.; Wong-Staal, F.; Gallo, R. C. Dexamethasone-Mediated Inhibition of Human T-cell Growth Factor and Gamma Interferon Messenger RNA. *J. Immunol.* **1984**, *133*, 273–276.
- Berger, A. S.; Cheng, C.-K.; Pearson, P. A.; Ashton, P.; Crooks, P. A.; Cynkowsky, T.; Cynkowska, G.; Jaffe, G. J. Intravitreal Sustained Release Corticosteroid-5-Fluorouracil Conjugate in the Treatment of Experimental Proliferative Vitreoretinopathy. *Invest. Ophthalmol. Visual Sci.* **1996**, *37*, 2318–2325.
- Staab, H. A. Synthesen mit Heterocyclischen Amidinen (Azolidinen). *Angew. Chem.* **1962**, *74*, 407–423.
- Yu, H. G.; Chung, H. Antiproliferative Effect of Mitomycin C on Experimental Proliferative Vitreoretinopathy in Rabbits. *Korean J. Ophthalmol.* **1997**, *11*, 98–105.
- Chandler, D. B.; Rozakis, G.; Dejaun, E.; Machermer, R. The Effect of Triamcinolone Acetonide on Refined Experimental Model of Proliferative Vitreoretinopathy. *Am. J. Ophthalmol.* **1985**, *99*, 686–690.
- Chandler, D. B.; Hida, T.; Sheta, S.; Proia, A. D.; Machermer, R. Improvement in Efficacy of Corticosteroid Therapy in an Animal Model of Proliferative Vitreoretinopathy by Pretreatment. *Graefes Arch. Clin. Exp. Ophthalmol.* **1987**, *225*, 259–265.
- Bernstein, S.; Lenhard, R. H.; Allen, W. S.; Heller, M.; Littell, R.; Stolar, S. M.; Feldman, L. I.; Blank, R. H. 16-Hydroxylated Steroids. VI. The Synthesis of the 16 α -Hydroxy Derivatives of 9 α -Substituted Steroids. *J. Am. Chem. Soc.* **1959**, *81*, 1689–1696.
- Organikum*, 18th ed.; Deutscher Verlag der Wissenschaften: Berlin, 1990; pp 396–408.
- Ishiki, N.; Onishi, H.; Machida, Y. Biological Properties of Conjugates of Mitomycin C with Estradiol Benzoate and Estradiol: Their Stability Characteristics in Biological Media and Their Binding Abilities to Estrogen Receptor. *Biol. Pharm. Bull.* **1997**, *20*, 1096–1102.
- Ishiki, N.; Onishi, H.; Machida, Y. Conversion Characteristics of the Conjugates of Mitomycin C with Estradiol and Estradiol Benzoate in Various pH Media. *Chem. Pharm. Bull.* **1997**, *45*, 1345–1349.
- Ishiki, N.; Onishi, H.; Machida, Y. In Vivo Properties of the Conjugates of Mitomycin C with Estradiol Benzoate and Estradiol: Pharmacokinetics and Antitumor Characteristics Against P388 Leukemia and Sarcoma 180. *Biol. Pharm. Bull.* **1998**, *21*, 1180–1186.
- Lyubarsky, A. L.; Pugh, E. N., Jr. Recovery Phase of the Murine Rod Photoresponse Reconstructed from Electroretinographic Recordings. *J. Neurosci.* **1996**, *16*, 563–571.
- Rohrer, B.; Korenbrot, J.; LaVail, M. M.; et al. Role of Neurotrophin Receptor TrkB in the Maturation of Rod Photoreceptors and Establishment of Synaptic Transmission to the Inner Retina. *J. Neurosci.* **1999**, *19*, 8919–8930.